Computers and Mathematics with Applications 61 (2011) 908–920

Contents lists available at ScienceDirect

Computers and Mathematics with Applications

journal homepage: www.elsevier.com/locate/camwa

Relaxation method for unsteady convection–diffusion equations

Wensheng Shen [a,*], Changjiang Zhang [b], Jun Zhang [b]

[a] Department of Computational Science, SUNY Brockport, Brockport, NY 14420, USA

[b] Department of Computer Science, University of Kentucky, Lexington, KY 40506–0046, USA

ARTICLE INFO

Article history:
Received 22 September 2010
Received in revised form 17 December 2010
Accepted 20 December 2010

Keywords:
Relaxation method
Convection-diffusion equation
WENO scheme
Implicit-explicit Runge–Kutta
Hyperbolic conservation laws

ABSTRACT

We propose and implement a relaxation method for solving unsteady linear and nonlinear convection–diffusion equations with continuous or discontinuity-like initial conditions. The method transforms a convection–diffusion equation into a relaxation system, which contains a stiff source term. The resulting relaxation system is then solved by a third-order accurate implicit–explicit (IMEX) Runge–Kutta method in time and a fifth-order finite difference WENO scheme in space. Numerical results show that the method can be used to effectively solve convection–diffusion equations with both smooth structures and discontinuities.

1. Introduction

Transport phenomena arise in many fields in industry, biology, agriculture, petrochemistry, and meteorology [1]. As a macroscale mathematical model, convection–diffusion equations, an important class of partial differential equations, have been widely used to describe these phenomena in science and engineering. However, due to various flow conditions and fluid properties, the solution to these equations presents serious numerical difficulties [2]. The one-dimensional (1D) convection–diffusion equation can be written as

$$\frac{\partial \phi}{\partial t} + u\frac{\partial \phi}{\partial x} - \mu\frac{\partial^2 \phi}{\partial x^2} = 0, \tag{1}$$

with an initial condition of $\phi(x, 0) = \phi_0(x)$. In Eq. (1), u is the velocity of convection and μ is the coefficient of viscosity. The above equation can be either convection or diffusion dominated, depending on the rate of convection of a physical quantity caused by flow and the rate of diffusion caused by gradient of the quantity, i.e. it becomes the heat equation or diffusion equation without convection ($u = 0$) and the wave equation without diffusion ($\mu = 0$). The impact of convection and diffusion on the transport of a physical quantity is measured by the cell Reynolds number or the local Peclet number (*Pe*), which is defined as the ratio of convective flux to diffusive flux,

$$Pe = \frac{u\Delta x}{\mu}, \tag{2}$$

where Δx is the grid spacing.

The changes of geometry and flow properties present serious challenges to numerical solution of convection–diffusion equations. Standard finite difference, finite volume, and finite element methods are not stable when the local numerical

* Corresponding author.
E-mail addresses: wshen@brockport.edu (W. Shen), czhanb@csr.uky.edu (C. Zhang), jzhang@cs.uky.edu (J. Zhang).
URL: http://www.cps.brockport.edu/~shen (W. Shen).

0898-1221/$ – see front matter
doi:10.1016/j.camwa.2010.12.039

Peclet number *Pe* is above 2 [3]. The standard methods generate solutions that exhibit non-physical oscillations and/or artificial numerical diffusions, which smear out sharp fronts of the solution where important chemistry and physics take place [4]. To resolve these difficulties, many specialized methods have been developed, including characteristic-based Eulerian methods [5–8], high order compact alternating direction implicit (ADI) methods [9–11], high order compact iterative methods [12,13], and high order Eulerian–Lagarangian localized adjoint methods [4]. The high order compact schemes [9,12,13,11] have successfully solved unsteady convection–diffusion equations under smooth conditions, where the initial condition is a smooth Gaussian pulse, but have not been tested with sharp discontinuities. The high order Eulerian–Lagarangian localized adjoint methods [4] have been reported to capture sharp fronts successfully, while in this paper we apply a new approach for solving convection–diffusion equations with discontinuities.

Characteristic-based Eulerian methods are relatively simple by using fixed spatial grids and practicing upstream weighting. As a result, the nonphysical oscillations present in the standard finite difference, finite volume, and finite element methods can be eliminated. Successful Eulerian methods are exampled by the TVD schemes [7,8] and the ENO/WENO schemes [14–16], which can resolve sharp discontinuities arising from the nonlinear hyperbolic conservation laws by incorporating characteristics. Traditionally, characteristic-based Eulerian methods solve the convection–diffusion equation by splitting it into two sub-steps, the convection step, which is solved explicitly by high order Eulerian schemes, and the diffusion step, which is solved implicitly by central difference [5,6]. Time accuracy of the Eulerian schemes, however, is deteriorated by the two-step splitting.

Motivated by Arora [3] and Arora and Roe [2], we propose using a relaxation method for the convection–diffusion equations, which are asymptotically transformed into equivalent relaxation systems. The relaxation method will significantly reduce the temporal truncation errors, allow large time steps in numerical simulations without loss of accuracy, and lead to a greatly improved efficiency. Several examples, including one-dimensional linear convection–diffusion equation, one-dimensional nonlinear convection–diffusion equation (the viscous Burgers' equation) with both smooth and sharp discontinuity-like initial conditions, and two-dimensional linear convection–diffusion equation, are conducted to test the accuracy of the proposed method. Our numerical results are compared with the exact solutions as well as those in published literatures.

2. The relaxation system in one dimension

The key of the relaxation method is to convert the original equation into its equivalent relaxation form. We construct the relaxation system by rewriting Eq. (1) as a system of two equations:

$$\frac{\partial \phi}{\partial t} + \frac{\partial \psi}{\partial x} = 0, \tag{3a}$$

$$\frac{\partial \psi}{\partial t} + \frac{\partial f(\phi)}{\partial x} = -\frac{1}{\tau}(\psi - g(\phi)). \tag{3b}$$

A new variable ψ is introduced in Eq. (3), and at equilibrium $\psi_{eq} = u - \mu \frac{\partial \phi}{\partial x}$. The actual forms of functions $f(\phi)$ and $g(\phi)$ are determined by the asymptotic analysis, which will be described below.

Following discussions in [3,17], we now let $\psi = g(\phi) + \psi_1$, where ψ_1 is a low frequency component. It is assumed that ψ_1 is small and its derivatives are negligible [3]. The temporal and spatial derivatives of ψ are

$$\frac{\partial \psi}{\partial t} = \frac{\partial g(\phi)}{\partial t} + \frac{\partial \psi_1}{\partial t}, \tag{4a}$$

$$\frac{\partial \psi}{\partial x} = \frac{\partial g(\phi)}{\partial x} + \frac{\partial \psi_1}{\partial x}. \tag{4b}$$

Neglecting the derivatives of ψ_1, Eqs. (4a) and (4b) can be simplified as

$$\frac{\partial \psi}{\partial t} = \frac{\partial g(\phi)}{\partial t} = \frac{\partial g(\phi)}{\partial \phi}\frac{\partial \phi}{\partial t}, \tag{5a}$$

$$\frac{\partial \psi}{\partial x} = \frac{\partial g(\phi)}{\partial x} = \frac{\partial g(\phi)}{\partial \phi}\frac{\partial \phi}{\partial x}. \tag{5b}$$

Substituting $\psi = g(\phi) + \psi_1$ into Eq. (3b), we have an expression for ψ_1

$$\psi_1 = -\tau\left(\frac{\partial \psi}{\partial t} + \frac{\partial f(\phi)}{\partial x}\right) = -\tau\left(\frac{\partial \psi}{\partial t} + \frac{\partial f(\phi)}{\partial \phi}\frac{\partial \phi}{\partial x}\right). \tag{6}$$

Substituting Eq. (5b) into Eq. (3a), we have

$$\frac{\partial \phi}{\partial t} = -\frac{\partial \psi}{\partial x} = -\frac{\partial g(\phi)}{\partial \phi}\frac{\partial \phi}{\partial x}. \tag{7}$$

Substituting Eq. (7) into Eq. (5a) gives the time derivative of ψ,

$$\frac{\partial\psi}{\partial t}=\frac{\partial g(\phi)}{\partial\phi}\frac{\partial\phi}{\partial t}=-\left(\frac{\partial g(\phi)}{\partial\phi}\right)^2\frac{\partial\phi}{\partial x}, \tag{8}$$

which is then substituted into Eq. (6) to find another expression for ψ_1,

$$\psi_1=-\tau\left(-\left(\frac{\partial g(\phi)}{\partial\phi}\right)^2\frac{\partial\phi}{\partial x}+\frac{\partial f(\phi)}{\partial\phi}\frac{\partial\phi}{\partial x}\right)=\tau\left(\left(\frac{\partial g(\phi)}{\partial\phi}\right)^2-\frac{\partial f(\phi)}{\partial\phi}\right)\frac{\partial\phi}{\partial x}. \tag{9}$$

Therefore the new expression for ψ is

$$\psi=g(\phi)+\psi_1=g(\phi)+\tau\left(\left(\frac{\partial g(\phi)}{\partial\phi}\right)^2-\frac{\partial f(\phi)}{\partial\phi}\right)\frac{\partial\phi}{\partial x}. \tag{10}$$

The desired asymptotic equation is then

$$\frac{\partial\phi}{\partial t}+\frac{\partial\psi}{\partial x}=\frac{\partial\phi}{\partial t}+\frac{\partial}{\partial x}\left(g(\phi)+\tau\left(\left(\frac{\partial g(\phi)}{\partial\phi}\right)^2-\frac{\partial f(\phi)}{\partial\phi}\right)\frac{\partial\phi}{\partial x}\right)=0, \tag{11}$$

or

$$\frac{\partial\phi}{\partial t}+\frac{\partial g(\phi)}{\partial x}+\tau\frac{\partial}{\partial x}\left(\left(\left(\frac{\partial g(\phi)}{\partial\phi}\right)^2-\frac{\partial f(\phi)}{\partial\phi}\right)\frac{\partial\phi}{\partial x}\right)=0. \tag{12}$$

The derived asymptotic equation, Eq. (12), must match the original convection–diffusion equation, Eq. (1). In linear cases, the advection velocity u is independent of the concentration ϕ. As a consequence, functions $g(\phi)$ and $f(\phi)$ must take the following form,

$$g(\phi)=u\phi \tag{13a}$$

$$f(\phi)=u^2\phi+\frac{\mu}{\tau}\phi. \tag{13b}$$

In nonlinear cases, such as the viscous Burgers' equation,

$$\frac{\partial u}{\partial t}+u\frac{\partial u}{\partial x}-\mu\frac{\partial^2 u}{\partial x^2}=0, \tag{14}$$

the corresponding asymptotic equation is

$$\frac{\partial u}{\partial t}+\frac{\partial g(u)}{\partial x}+\tau\frac{\partial}{\partial x}\left(\left(\left(\frac{\partial g(u)}{\partial u}\right)^2-\frac{\partial f(u)}{\partial u}\right)\frac{\partial u}{\partial x}\right)=0, \tag{15}$$

and functions $f(u)$ and $g(u)$ must take the form

$$g(u)=\frac{1}{2}u^2 \tag{16a}$$

$$f(u)=\frac{1}{3}u^3+\frac{\mu}{\tau}u. \tag{16b}$$

Therefore, for one-dimensional convection–diffusion equation with constant advection velocity, the final form of the relaxation system is

$$\frac{\partial\phi}{\partial t}+\frac{\partial\psi}{\partial x}=0, \tag{17a}$$

$$\frac{\partial\psi}{\partial t}+\left(u^2+\frac{\mu}{\tau}\right)\frac{\partial\phi}{\partial x}=-\frac{\psi-u\phi}{\tau}. \tag{17b}$$

The relaxation system, Eq. (17), is equivalent to the original convection–diffusion equation asymptotically [3,2]. We thus transform the one-dimensional convection–diffusion equation to a relaxation system of two equations. In the rest of the paper, we will describe how to solve the relaxation system using high-order accurate characteristic-based methods for solving hyperbolic conservation laws.

3. Characteristics of the relaxation system

We rewrite Eq. (17) in the following vector form

$$\frac{\partial \vec{U}}{\partial t}+\frac{\partial \vec{E}}{\partial x}=\vec{S}, \tag{18}$$

where $\vec{U}$, $\vec{E}$, and $\vec{S}$ are the unknown vector, flux vector, and source vector, respectively, defined by

$$\vec{U}=\begin{Bmatrix}\phi\\ \psi\end{Bmatrix}\qquad \vec{E}=\begin{Bmatrix}\psi\\ \left(\frac{\mu}{\tau}+u^2\right)\phi\end{Bmatrix}\qquad \vec{S}=\begin{Bmatrix}0\\ -\frac{1}{\tau}(\psi-u\phi)\end{Bmatrix}. \tag{19}$$

We write Eq. (18) in matrix–vector product form,

$$\frac{\partial \vec{U}}{\partial t}+A\frac{\partial \vec{U}}{\partial x}=\vec{S}, \tag{20}$$

where A is a 2×2 matrix, defined as

$$A=\begin{pmatrix}0 & 1\\ \frac{\mu}{\tau}+u^2 & 0\end{pmatrix}. \tag{21}$$

We decompose matrix A such that $A=R\Lambda R^{-1}$, where matrices R, Λ, and R^{-1} are defined by

$$R=\begin{pmatrix}\frac{1}{\sqrt{\frac{\mu}{\tau}+u^2}} & -\frac{1}{\sqrt{\frac{\mu}{\tau}+u^2}}\end{pmatrix},\qquad \Lambda=\begin{pmatrix}\lambda_1 & 0\\ 0 & \lambda_2\end{pmatrix},\quad \text{and}\quad R^{-1}=\begin{pmatrix}\frac{1}{2} & \frac{1}{2\sqrt{\frac{\mu}{\tau}+u^2}}\\ \frac{1}{2} & -\frac{1}{2\sqrt{\frac{\mu}{\tau}+u^2}}\end{pmatrix}, \tag{22}$$

where $\lambda_1=\sqrt{\frac{\mu}{\tau}+u^2}$ and $\lambda_2=-\sqrt{\frac{\mu}{\tau}+u^2}$.

A new set of system of equations is obtained by multiplying Eq. (20) with R^{-1},

$$\frac{\partial \vec{W}}{\partial t}+\Lambda\frac{\partial \vec{W}}{\partial x}=\vec{\Theta}, \tag{23}$$

where the characteristics $\vec{W}$ is defined as $\vec{W}=R^{-1}\vec{U}$, and the new source term is defined as $\vec{\Theta}=R^{-1}\vec{S}$. We notice that the initial relaxation system is coupled, while the new system, Eq. (23), contains two independent characteristics, $W_1=\frac{1}{2}\phi+\frac{\psi}{2\sqrt{\frac{\mu}{\tau}+u^2}}$ and $W_2=\frac{1}{2}\phi-\frac{\psi}{2\sqrt{\frac{\mu}{\tau}+u^2}}$, where W_1 travels from left to right corresponding to the positive eigenvalue $\lambda_1=\sqrt{\frac{\mu}{\tau}+u^2}$, and W_2 travels from right to left corresponding to the negative eigenvalue $\lambda_2=-\sqrt{\frac{\mu}{\tau}+u^2}$. The components of the new source term are $\Theta_1=-\frac{\psi}{2\sqrt{\mu\tau+u^2\tau^2}}+\frac{u\phi}{2\sqrt{\mu\tau+u^2\tau^2}}$ and $\Theta_2=\frac{\psi}{2\sqrt{\mu\tau+u^2\tau^2}}-\frac{u\phi}{2\sqrt{\mu\tau+u^2\tau^2}}$. Many numerical methods designed for hyperbolic conservation laws can be applied to solve Eq. (23), such as high resolution TVD (Total Variation Diminishing) schemes [7,8], and high order WENO schemes [14]. Here, we propose to use high order WENO schemes, since they are good for problems that involve both sharp discontinuities and rich smooth structures [16].

4. A fifth order finite difference WENO scheme

Various high-order WENO schemes have been proposed since their appearance, including cell average based finite volume schemes [15], and point value based finite difference ones [14]. We apply the fifth order finite difference WENO scheme developed by Jiang and Shu [14], which is recalled here for convenience. We start with Eq. (23), and write it in a scalar form,

$$\frac{\partial W_k}{\partial t}+\lambda_k\frac{\partial W_k}{\partial x}=\Theta_k, \tag{24}$$

where W_k indicates the kth components of vector $\vec{W}$, and λ_k is the corresponding kth eigenvalue of matrix A. Contrary to the original work of the fifth-order finite difference WENO scheme [14], where no source term is present in their equation of conservation laws, here a non-trivial source term is included in our relaxation system of Eq. (24). Let $\Delta t=t^{n+1}-t^n$ and $\Delta x=x_{j+1}-x_j$, Eq. (24) may be discretized in finite difference as

$$\frac{\partial W_k}{\partial t}=-\frac{1}{\Delta x}\left(f_{i+\frac{1}{2}}-f_{i-\frac{1}{2}}\right)+\Theta_k, \tag{25}$$

where $f = \lambda_k W_k$. Introducing an operator $L(W_k)$,

$$L(W_k) = -\frac{1}{\Delta x}\left(f_{i+\frac{1}{2}} - f_{i-\frac{1}{2}}\right) + \Theta_k, \tag{26}$$

we may discretize Eq. (25) in time by the classic third-order TVD Runge–Kutta scheme [14]

$$W_k^{(1)} = W_k^n + \Delta t L(W_k^n), \tag{27a}$$

$$W_k^{(2)} = \frac{3}{4}W_k^n + \frac{1}{4}W_k^{(1)} + \frac{1}{4}\Delta t L(W_k^{(1)}), \tag{27b}$$

$$W_k^{n+1} = \frac{1}{3}W_k^n + \frac{2}{3}W_k^{(2)} + \frac{2}{3}\Delta t L(W_k^{(2)}). \tag{27c}$$

The numerical scheme, Eq. (27), is stable when

$$CFL = \left|\lambda_k \frac{\Delta t}{\Delta x}\right| \le 1. \tag{28}$$

The numerical flux $f_{j+\frac{1}{2}}$ is constructed by the fifth-order WENO reconstruction,

$$f_{j+\frac{1}{2}} \approx \sum_{i=0}^{2} \omega_i p_i\left(x_{j+\frac{1}{2}}\right), \tag{29}$$

where ω_i is the weight, and $p_i(x_{j+\frac{1}{2}})$ is the second-order polynomial on stencil S_i. For right-traveling wave, λ_k is positive, the polynomials are constructed as [14],

$$p_0\left(x_{j+\frac{1}{2}}\right) = \frac{2}{6}f(x_{j-2}) - \frac{7}{6}f(x_{j-1}) + \frac{11}{6}f(x_j), \tag{30a}$$

$$p_1\left(x_{j+\frac{1}{2}}\right) = -\frac{1}{6}f(x_{j-1}) + \frac{5}{6}f(x_j) + \frac{2}{6}f(x_{j+1}), \tag{30b}$$

$$p_2\left(x_{j+\frac{1}{2}}\right) = \frac{2}{6}f(x_j) + \frac{5}{6}f(x_{j+1}) - \frac{1}{6}f(x_{j+2}). \tag{30c}$$

The scaled weight ω_i in Eq. (29) is calculated as

$$\omega_i = \frac{\bar{\omega}_i}{\sum\limits_{i=0,2} \bar{\omega}_i}, \tag{31}$$

where $\bar{\omega}_i$ is the nonlinear weight, based on the smoothness indicator β_i,

$$\bar{\omega}_i = \frac{\gamma_i}{(\epsilon + \beta_i)^2}, \tag{32}$$

where ϵ is a small number to prevent dividing by zero, i.e. $\epsilon = 10^{-10}$, and the smoothness indicator β_i for each stencil S_i is

$$\beta_0 = \frac{13}{12}(f(x_{j-2}) - 2f(x_{j-1}) + f(x_j))^2 + \frac{1}{4}(f(x_{j-2}) - 4f(x_{j-1}) + 3f(x_j))^2, \tag{33a}$$

$$\beta_1 = \frac{13}{12}(f(x_{j-1}) - 2f(x_j) + f(x_{j+1}))^2 + \frac{1}{4}(f(x_{j-1}) - f(x_{j+1}))^2, \tag{33b}$$

$$\beta_2 = \frac{13}{12}(f(x_j) - 2f(x_{j+1}) + f(x_{j+2}))^2 + \frac{1}{4}(3f(x_j) - 4f(x_{j+1}) + f(x_{j+2}))^2. \tag{33c}$$

The linear weights in Eq. (32) are determined by

$$\gamma_0 = \frac{1}{10}, \qquad \gamma_1 = \frac{6}{10}, \quad \text{and} \quad \gamma_2 = \frac{3}{10}. \tag{34}$$

5. Time discretization by IMEX Runge–Kutta methods

For stability consideration, the relaxation system must satisfy Liu's sub-characteristic condition [17], which gives a constraint on the relaxation parameter τ [3],

$$\tau \leq \frac{\mu}{u^2}. \tag{35}$$

Arora [3] suggested that τ should be chosen to be a little smaller than the maximum allowable value, i.e. 70% of $\frac{\mu}{u^2}$. The three-stage third-order explicit TVD Runge–Kutta scheme, introduced in Section 4, works when the viscous coefficient is large enough, i.e. $Pe <= 4.0$, and τ is taken as the suggested value. When the viscous coefficient is smaller, so does the relaxation parameter, the resulting relaxation system, however, becomes stiff, and the standard third-order explicit TVD Runge–Kutta scheme cannot produce the desired solution. We therefore, apply the implicit–explicit (IMEX) Runge–Kutta methods, proposed by Pareschi and Russo [18], to the relaxation system, Eq. (18), which may be rewritten as

$$\frac{\partial \vec{U}}{\partial t} + \frac{\partial \vec{E}(\vec{U})}{\partial x} = \frac{1}{\tau}\vec{Q}(\vec{U}), \tag{36}$$

where $\vec{Q}(\vec{U}) = (0, u\phi - \psi)^T$. We use the third-order strong-stability-preserving (SSP) scheme, where the implicit part is treated by an L-stable diagonally implicit Runge–Kutta [18]. The 4-stage scheme can be summarized as [18]

$$\vec{U}^i = \vec{U}^n - \Delta t \sum_{j=1}^{i-1} \tilde{a}_{ij} \frac{\partial \vec{E}(\vec{U}^j)}{\partial x} + \Delta t \sum_{j=1}^{4} a_{ij} \frac{1}{\tau}\vec{Q}(\vec{U}^j), \tag{37a}$$

$$\vec{U}^{n+1} = \vec{U}^n - \Delta t \sum_{i=1}^{4} \tilde{\omega}_i \frac{\partial \vec{E}(\vec{U}^i)}{\partial x} + \Delta t \sum_{i=1}^{4} \omega_i \frac{1}{\tau}\vec{Q}(\vec{U}^i), \tag{37b}$$

where i indicates the four stages, $i = 1$–4, and the 4-element vectors $\tilde{\omega}$ and ω are defined as $\tilde{\omega} = (0, 1/6, 1/6, 2/3)^T$ and $\omega = (0, 1/6, 1/6, 2/3)^T$, respectively. In Eqs. (37a) and (37b), $\tilde{a}_{ij}$ and a_{ij} are elements of the 4×4 matrices $\tilde{A}$ and A, which can be written as

$$\tilde{A} = \begin{pmatrix} 0 & 0 & 0 & 0 \\ 0 & 0 & 0 & 0 \\ 0 & 1 & 0 & 0 \\ 0 & 1/4 & 1/4 & 0 \end{pmatrix} \quad \text{and} \quad A = \begin{pmatrix} \alpha & 0 & 0 & 0 \\ -\alpha & \alpha & 0 & 0 \\ 0 & 1-\alpha & \alpha & 0 \\ \beta & \eta & 1/2-\beta-\eta-\alpha & \alpha \end{pmatrix}, \tag{38}$$

where, $\alpha = 0.241694260788221$, $\beta = 0.06042356519705$, and $\eta = 0.12915286960590$. As a demonstration, the first two stages of the scheme are

$$\vec{U}^1 = \vec{U}^n + \Delta t a_{11} \frac{1}{\tau}\vec{Q}(\vec{U}^1), \tag{39a}$$

$$\vec{U}^2 = \vec{U}^n + \Delta t a_{21} \frac{1}{\tau}\vec{Q}(\vec{U}^1) + \Delta t a_{22} \frac{1}{\tau}\vec{Q}(\vec{U}^2), \tag{39b}$$

where only $\vec{U}^1$ terms are implicit in Eq. (39a), so are $\vec{U}^2$ terms in Eq. (39b). To solve the equations, we play simple algebra by moving the diagonally implicit terms in Eqs. (37a) and (37b) from the right-hand side to the left-hand side.

6. Extension to two-dimension

6.1. Asymptotic analysis

We now discuss how to extend the method to multi-dimensions. It is assumed that diffusion is isotropic. A two-dimensional convection–diffusion equation can be written as

$$\frac{\partial \phi}{\partial t} + u\frac{\partial \phi}{\partial x} + v\frac{\partial \phi}{\partial y} - \mu\frac{\partial^2 \phi}{\partial x^2} - \mu\frac{\partial^2 \phi}{\partial y^2} = 0, \tag{40}$$

where u and v are the velocities in the x and y directions, respectively. Introducing variables ψ and φ, the corresponding relaxation equations are then taking the form

$$\frac{\partial \phi}{\partial t} + \frac{\partial \psi}{\partial x} + \frac{\partial \varphi}{\partial y} = 0, \tag{41a}$$

$$\frac{\partial \psi}{\partial t} + \frac{\partial f(\phi)}{\partial x} = -\frac{1}{\tau}(\psi - g(\phi)), \tag{41b}$$

$$\frac{\partial \varphi}{\partial t} + \frac{\partial p(\phi)}{\partial y} = -\frac{1}{\tau}(\varphi - q(\phi)). \tag{41c}$$

Following similar procedures in Section 2, we let $\psi = g(\phi) + \psi_1$ and $\varphi = q(\phi) + \varphi_1$, where low frequency components ψ_1 and φ_1 are assumed to be very small and their derivatives are even smaller. We take the derivatives of ψ with respect to t or x, and those of φ with respect to t or y, omit the derivatives of ψ_1 and φ_1, and obtain the simplified temporal and spatial derivatives of ψ and φ,

$$\frac{\partial \psi}{\partial t} = \frac{\partial g(\phi)}{\partial \phi}\frac{\partial \phi}{\partial t}, \tag{42a}$$

$$\frac{\partial \psi}{\partial x} = \frac{\partial g(\phi)}{\partial \phi}\frac{\partial \phi}{\partial x}, \tag{42b}$$

$$\frac{\partial \varphi}{\partial t} = \frac{\partial q(\phi)}{\partial \phi}\frac{\partial \phi}{\partial t}, \tag{42c}$$

$$\frac{\partial \varphi}{\partial y} = \frac{\partial q(\phi)}{\partial \phi}\frac{\partial \phi}{\partial y}. \tag{42d}$$

We then substitute $\psi = g(\phi) + \psi_1$ and $\varphi = q(\phi) + \varphi_1$ into Eqs. (41b) and (41c), and obtain the expressions about ψ_1 in terms of ψ and $f(\phi)$ and φ_1 in terms of φ and $p(\phi)$, respectively,

$$\psi_1 = -\tau\left(\frac{\partial \psi}{\partial t} + \frac{\partial f(\phi)}{\partial x}\right) \quad \text{and} \quad \varphi_1 = -\tau\left(\frac{\partial \varphi}{\partial t} + \frac{\partial p(\phi)}{\partial y}\right). \tag{43}$$

The spatial derivatives of ψ and φ, Eqs. (42b) and (42d), are substituted into Eq. (41a) to obtain an alternative expression for $\frac{\partial \phi}{\partial t}$,

$$\frac{\partial \phi}{\partial t} = -\left(\frac{\partial g(\phi)}{\partial \phi}\frac{\partial \phi}{\partial x} + \frac{\partial q(\phi)}{\partial \phi}\frac{\partial \phi}{\partial y}\right). \tag{44}$$

Substituting Eq. (44) into Eqs. (42a) and (42c), we update the temporal derivatives of ψ and φ as

$$\frac{\partial \psi}{\partial t} = -\frac{\partial g(\phi)}{\partial \phi}\left(\frac{\partial g(\phi)}{\partial \phi}\frac{\partial \phi}{\partial x} + \frac{\partial q(\phi)}{\partial \phi}\frac{\partial \phi}{\partial y}\right), \tag{45a}$$

$$\frac{\partial \varphi}{\partial t} = -\frac{\partial q(\phi)}{\partial \phi}\left(\frac{\partial g(\phi)}{\partial \phi}\frac{\partial \phi}{\partial x} + \frac{\partial q(\phi)}{\partial \phi}\frac{\partial \phi}{\partial y}\right), \tag{45b}$$

which are then substituted into Eq. (43) for ψ_1 and φ_1,

$$\begin{aligned}\psi_1 &= -\tau\left(-\left(\frac{\partial g(\phi)}{\partial \phi}\right)^2\frac{\partial \phi}{\partial x} - \frac{\partial g(\phi)}{\partial \phi}\frac{\partial q(\phi)}{\partial \phi}\frac{\partial \phi}{\partial y} + \frac{\partial f(\phi)}{\partial x}\right)\\ &= \tau\left(\left(\frac{\partial g(\phi)}{\partial \phi}\right)^2 - \frac{\partial f(\phi)}{\partial \phi}\right)\frac{\partial \phi}{\partial x} + \tau\frac{\partial g(\phi)}{\partial \phi}\frac{\partial q(\phi)}{\partial \phi}\frac{\partial \phi}{\partial y},\end{aligned} \tag{46a}$$

$$\begin{aligned}\varphi_1 &= -\tau\left(-\frac{\partial q(\phi)}{\partial \phi}\frac{\partial g(\phi)}{\partial \phi}\frac{\partial \phi}{\partial x} - \left(\frac{\partial q(\phi)}{\partial \phi}\right)^2\frac{\partial \phi}{\partial y} + \frac{\partial p(\phi)}{\partial y}\right)\\ &= \tau\left(\left(\frac{\partial q(\phi)}{\partial \phi}\right)^2 - \frac{\partial p(\phi)}{\partial \phi}\right)\frac{\partial \phi}{\partial y} + \tau\frac{\partial q(\phi)}{\partial \phi}\frac{\partial g(\phi)}{\partial \phi}\frac{\partial \phi}{\partial x}.\end{aligned} \tag{46b}$$

Therefore the new expressions for ψ and φ are derived as

$$\begin{aligned}\psi &= g(\phi) + \psi_1\\ &= g(\phi) + \tau\left(\left(\frac{\partial g(\phi)}{\partial \phi}\right)^2 - \frac{\partial f(\phi)}{\partial \phi}\right)\frac{\partial \phi}{\partial x} + \tau\frac{\partial g(\phi)}{\partial \phi}\frac{\partial q(\phi)}{\partial \phi}\frac{\partial \phi}{\partial y},\end{aligned} \tag{47a}$$

$$\begin{aligned}\varphi &= q(\phi) + \varphi_1\\ &= q(\phi) + \tau\left(\left(\frac{\partial q(\phi)}{\partial \phi}\right)^2 - \frac{\partial p(\phi)}{\partial \phi}\right)\frac{\partial \phi}{\partial y} + \tau\frac{\partial q(\phi)}{\partial \phi}\frac{\partial g(\phi)}{\partial \phi}\frac{\partial \phi}{\partial x}.\end{aligned} \tag{47b}$$

Finally, we obtain the desired asymptotic counterpart for the two-dimensional convection–diffusion equation,

$$\frac{\partial \phi}{\partial t}+\frac{\partial \psi}{\partial x}+\frac{\partial \varphi}{\partial y} = \frac{\partial \phi}{\partial t}+\frac{\partial}{\partial x}\left(g(\phi)+\tau\left(\left(\frac{\partial g(\phi)}{\partial \phi}\right)^2-\frac{\partial f(\phi)}{\partial \phi}\right)\frac{\partial \phi}{\partial x}+\tau\frac{\partial g(\phi)}{\partial \phi}\frac{\partial q(\phi)}{\partial \phi}\frac{\partial \phi}{\partial y}\right)$$
$$+\frac{\partial}{\partial y}\left(q(\phi)+\tau\left(\left(\frac{\partial q(\phi)}{\partial \phi}\right)^2-\frac{\partial p(\phi)}{\partial \phi}\right)\frac{\partial \phi}{\partial y}+\tau\frac{\partial q(\phi)}{\partial \phi}\frac{\partial g(\phi)}{\partial \phi}\frac{\partial \phi}{\partial x}\right)=0, \tag{48}$$

or

$$\frac{\partial \phi}{\partial t}+\frac{\partial g(\phi)}{\partial x}+\frac{\partial q(\phi)}{\partial y} = -\tau\frac{\partial}{\partial x}\left(\left(\left(\frac{\partial g(\phi)}{\partial \phi}\right)^2-\frac{\partial f(\phi)}{\partial \phi}\right)\frac{\partial \phi}{\partial x}\right)-\tau\frac{\partial}{\partial x}\left(\frac{\partial g(\phi)}{\partial \phi}\frac{\partial q(\phi)}{\partial \phi}\frac{\partial \phi}{\partial y}\right)$$
$$-\tau\frac{\partial}{\partial y}\left(\left(\left(\frac{\partial q(\phi)}{\partial \phi}\right)^2-\frac{\partial p(\phi)}{\partial \phi}\right)\frac{\partial \phi}{\partial y}\right)-\tau\frac{\partial}{\partial y}\left(\frac{\partial q(\phi)}{\partial \phi}\frac{\partial g(\phi)}{\partial \phi}\frac{\partial \phi}{\partial x}\right). \tag{49}$$

We ignore the cross-derivative terms in Eq. (49), for diffusion is assumed to be isotropic. For the convection–diffusion equation with constant advection velocity, the following conditions must be satisfied,

$$g(\phi)=u\phi, \qquad \mu=-\tau\left(\left(\frac{\partial g(\phi)}{\partial \phi}\right)^2-\frac{\partial f(\phi)}{\partial \phi}\right), \tag{50a}$$

$$q(\phi)=v\phi, \qquad \mu=-\tau\left(\left(\frac{\partial q(\phi)}{\partial \phi}\right)^2-\frac{\partial p(\phi)}{\partial \phi}\right). \tag{50b}$$

Rearranging Eqs. (50a) and (50b) and integrating $f(\phi)$ and $p(\phi)$ versus ϕ, functions $f(\phi)$ and $p(\phi)$ should have the form of

$$f(\phi)=u^2\phi+\frac{\mu}{\tau}\phi, \tag{51a}$$

$$p(\phi)=v^2\phi+\frac{\mu}{\tau}\phi. \tag{51b}$$

6.2. Characteristics of two-dimensional system

We rewrite Eqs. (41a)–(41c) in vector form as

$$\frac{\partial \vec{U}}{\partial t}+\frac{\partial \vec{E}}{\partial x}+\frac{\partial \vec{F}}{\partial y}=\vec{S}, \tag{52}$$

where the vectors are defined as

$$\vec{U}=\begin{Bmatrix}\phi\\ \psi\\ \varphi\end{Bmatrix}, \qquad \vec{E}=\begin{Bmatrix}\psi\\ \left(\frac{\mu}{\tau}+u^2\right)\phi\\ 0\end{Bmatrix}, \qquad \vec{F}=\begin{Bmatrix}\varphi\\ 0\\ \left(\frac{\mu}{\tau}+v^2\right)\phi\end{Bmatrix}, \quad \text{and} \quad \vec{S}=\begin{Bmatrix}0\\ -\frac{1}{\tau}(\psi-u\phi)\\ -\frac{1}{\tau}(\varphi-v\phi)\end{Bmatrix}. \tag{53}$$

We decouple Eq. (52) by calculating the Jacobian matrices $A=\frac{\partial \vec{E}}{\partial \vec{U}}$ and $B=\frac{\partial \vec{F}}{\partial \vec{U}}$, and write Eq. (52) in matrix–vector product form,

$$\frac{\partial \vec{U}}{\partial t}+A\frac{\partial \vec{U}}{\partial x}+B\frac{\partial \vec{U}}{\partial y}=\vec{S}, \tag{54}$$

where the matrices A and B are defined as

$$A=\begin{pmatrix}0 & 1 & 0\\ \frac{\mu}{\tau}+u^2 & 0 & 0\\ 0 & 0 & 0\end{pmatrix} \quad \text{and} \quad B=\begin{pmatrix}0 & 0 & 1\\ 0 & 0 & 0\\ \frac{\mu}{\tau}+v^2 & 0 & 0\end{pmatrix}. \tag{55}$$

We further decompose matrices A and B into diagonal form $A=R_A\Lambda_AR_A^{-1}$ and $B=R_B\Lambda_BR_B^{-1}$, and rewrite Eq. (54) in the form,

$$\frac{\partial \vec{U}}{\partial t}+R_A\Lambda_AR_A^{-1}\frac{\partial \vec{U}}{\partial x}+R_B\Lambda_BR_B^{-1}\frac{\partial \vec{U}}{\partial y}=\vec{S}, \tag{56}$$

where R_A and R_B and the matrices of eigenvectors, and Λ_A and Λ_B are the matrices of eigenvalues. The matrices R_A, Λ_A, and R_A^{-1} are defined as

$$R_A = \begin{pmatrix} 0 & 1 & 1 \\ 0 & \lambda_2 & \lambda_3 \\ 1 & 0 & 0 \end{pmatrix}, \qquad \Lambda_A = \begin{pmatrix} \lambda_1 & 0 & 0 \\ 0 & \lambda_2 & 0 \\ 0 & 0 & \lambda_3 \end{pmatrix}, \quad \text{and} \quad R_A^{-1} = \begin{pmatrix} 0 & 0 & 1 \\ \frac{1}{2} & \frac{1}{2\sqrt{\frac{\mu}{\tau}+u^2}} & 0 \\ \frac{1}{2} & -\frac{1}{2\sqrt{\frac{\mu}{\tau}+u^2}} & 0 \end{pmatrix}, \tag{57}$$

where, $\lambda_1 = 0$, $\lambda_2 = \sqrt{\frac{\mu}{\tau}+u^2}$, and $\lambda_3 = -\sqrt{\frac{\mu}{\tau}+u^2}$. Similarly, matrices R_B, Λ_B, and R_B^{-1} are defined as

$$R_B = \begin{pmatrix} 0 & 1 & 1 \\ 1 & 0 & 0 \\ 0 & \lambda_2 & \lambda_3 \end{pmatrix}, \qquad \Lambda_B = \begin{pmatrix} \lambda_1 & 0 & 0 \\ 0 & \lambda_2 & 0 \\ 0 & 0 & \lambda_3 \end{pmatrix}, \quad \text{and} \quad R_B^{-1} = \begin{pmatrix} 0 & 1 & 0 \\ \frac{1}{2} & 0 & \frac{1}{2\sqrt{\frac{\mu}{\tau}+v^2}} \\ \frac{1}{2} & 0 & -\frac{1}{2\sqrt{\frac{\mu}{\tau}+v^2}} \end{pmatrix}, \tag{58}$$

where $\lambda_1 = 0$, $\lambda_2 = \sqrt{\frac{\mu}{\tau}+v^2}$, and $\lambda_3 = -\sqrt{\frac{\mu}{\tau}+v^2}$. The characteristics in the x- and y-coordinates, $\vec{W}_A$ and $\vec{W}_B$, are calculated, respectively, as

$$\vec{W}_A = R_A^{-1}\vec{U} \quad \text{and} \quad \vec{W}_B = R_B^{-1}\vec{U}. \tag{59}$$

6.3. Numerical implementation

We tried to apply a first-order temporal and second-order spatial TVD scheme [7,8] to the two-dimensional relaxation system, but the solution was not acceptable. We also tried to extend the third-order TVD WENO scheme [14] to two-dimension by the fractional-step method [19], i.e.,

$$\frac{\partial \vec{U}}{\partial t} + \frac{\partial \vec{E}}{\partial x} = \frac{1}{2}\vec{S}, \tag{60a}$$

$$\frac{\partial \vec{U}}{\partial t} + \frac{\partial \vec{F}}{\partial y} = \frac{1}{2}\vec{S}, \tag{60b}$$

but obtained only undesirable results. We then implement the extension via the dimension-by-dimension approach,

$$\frac{\vec{U}_{i,j}^{n+1} - \vec{U}_{i,j}^{n}}{\Delta t} = -\frac{1}{\Delta x}\left(f_{i+\frac{1}{2},j} - f_{i-\frac{1}{2},j}\right) - \frac{1}{\Delta y}\left(g_{i,j+\frac{1}{2}} - g_{i,j-\frac{1}{2}}\right) + \vec{S}, \tag{61}$$

where numerical fluxes are calculated as

$$f_{i+\frac{1}{2},j} = \left(R_A \Lambda_A \vec{W}_A\right)_{i+\frac{1}{2},j} \quad \text{and} \quad g_{i,j+\frac{1}{2}} = \left(R_B \Lambda_B \vec{W}_B\right)_{i,j+\frac{1}{2}}. \tag{62}$$

The fifth-order WENO reconstruction procedure described in Section 4 is applied to each characteristic for space discretization. Again, we use the third-order strong stability preserving IMEX Runge–Kutta [18] for time discretization.

7. Numerical examples

Example 1. One-dimension with constant velocity.

We solve Eq. (1) using the proposed relaxation method and the fifth-order WENO scheme, and compare the numerical results with an analytical solution, which was found by Noye and Tan [12],

$$\phi(x,t) = \frac{1}{\sqrt{4t+1}} \exp\left(-\frac{(x-1-ut)^2}{\mu(4t+1)}\right). \tag{63}$$

The initial condition corresponding to Eq. (63) is

$$\phi(x,0) = \exp\left(-\frac{(x-1)^2}{\mu}\right), \quad 0 \le x \le 9. \tag{64}$$

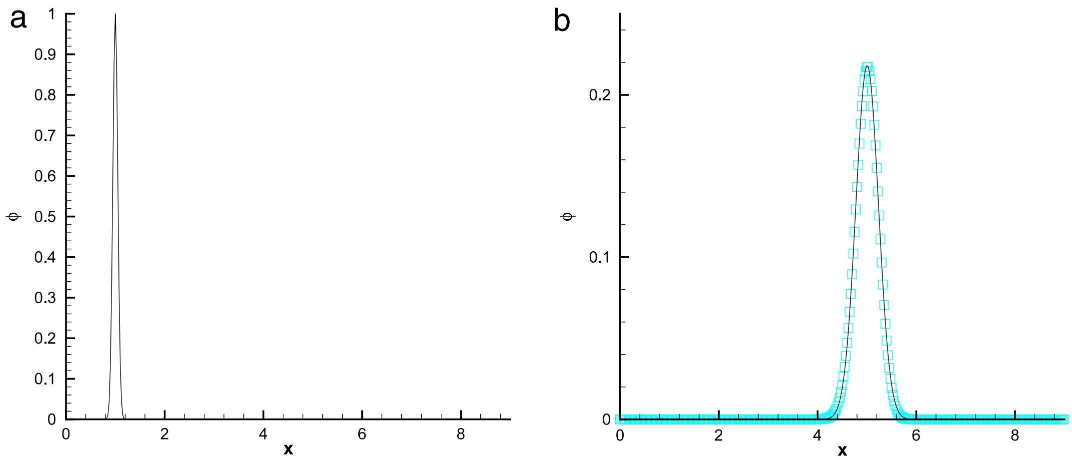

Fig. 1. Solution of 1D convection–diffusion equation by relaxation method (a) Initial condition in Gaussian distribution. (b) Concentration distribution at $t = 5$ s, where the solid line is the analytical solution, and squares indicate the numerical solution.

Table 1
Dependence of accuracy on problem size.

Case	N	Δx	Δt	Pe	L_1 error	L_∞ error
1	90	0.1	0.03904	16.0	3.460×10^{-3}	4.585×10^{-2}
2	180	0.05	0.01952	8.0	5.551×10^{-4}	8.848×10^{-3}
3	360	0.025	0.00976	4.0	2.685×10^{-4}	3.120×10^{-3}
4	720	0.0125	0.00488	2.0	2.702×10^{-4}	3.001×10^{-3}

The boundary conditions corresponding to the solution are

$$\phi(0,t) = \frac{1}{\sqrt{4t+1}} \exp\left(-\frac{(ut+1)^2}{\mu(4t+1)}\right), \tag{65}$$

and

$$\phi(9,t) = \frac{1}{\sqrt{4t+1}} \exp\left(-\frac{(8-ut)^2}{\mu(4t+1)}\right). \tag{66}$$

Numerical results on this problem are presented in Table 1, corresponding to the condition of $u = 0.8$, $\mu = 0.005$, and $\tau = 0.005$. For the four tested mesh sizes, our method is fairly stable. In a coarse grid, $\Delta x = 0.1$, L_1 error is 3.460×10^{-3}. When dx is halved, L_1 error sharply decreases to 5.551×10^{-4}, one order of magnitude lower. When mesh size is increased to $N = 720$, L_1 error stagnates. The accuracy of our method, however, can be improved by adjusting the value of τ, as shown in Table 2. When the relaxation parameter decreases from $\tau = 0.005$ to $\tau = 0.0001$, L_1 error decreases from 2.702×10^{-4} to 7.502×10^{-6}. A graphic comparison between the analytical and numerical solutions is presented in Fig. 1, where Fig. 1(a) is the profile of the initial Gaussian pulse, while Fig. 1(b) is the profile of Gaussian pulse at $t = 5.0$, corresponding to $\mu = 0.005$, $N = 360$, $Pe = 4.0$, and $\Delta t = 0.00976$. The solid line in Fig. 1(b) represents the analytical solution, while the square symbols indicate results from numerical calculation. It can be clearly observed from Fig. 1(b) that our numerical results agree with the analytical solution very well. The advantage of the proposed numerical method for solving convection–diffusion equation is further demonstrated by its ability to handle small viscous coefficient. In our numerical test, we use $\mu = 0.00025$, $N = 720$, and $Pe = 40.0$, and the solution is still fairly accurate, L_1 error being 3.601×10^{-4} and L_∞ error being 2.094×10^{-2}.

Example 2. One-dimensional viscous Burgers' equation.

To test the ability of the proposed method for nonlinear problems, we apply it to a one-dimensional viscous Burgers' equation, Eq. (14). The relaxation form of Eq. (14) is given as

$$\frac{\partial u}{\partial t} + \frac{\partial \psi}{\partial x} = 0, \tag{67a}$$

$$\frac{\partial \psi}{\partial t} + \left(u^2 + \frac{\mu}{\tau}\right)\frac{\partial u}{\partial x} = -\frac{\psi - \frac{1}{2}u^2}{\tau}. \tag{67b}$$

Table 2
Dependence of accuracy on relaxation parameter.

Case	N	Δx	τ	Δt	Pe	L_1 error	L_∞ error
1	720	0.0125	0.005	4.880×10^{-3}	2.0	2.702×10^{-4}	3.001×10^{-3}
2	720	0.0125	0.001	2.632×10^{-3}	2.0	5.402×10^{-5}	5.969×10^{-4}
3	720	0.0125	0.0005	1.916×10^{-3}	2.0	2.649×10^{-5}	3.075×10^{-4}
4	720	0.0125	0.0001	8.783×10^{-4}	2.0	7.502×10^{-6}	1.248×10^{-4}

Table 3
Dependence of accuracy on viscous coefficient for the Burgers' equation.

Case	Δx	Δt	t	$\mu = 0.05$		$\mu = 0.005$	
				L_1 error	L_∞ error	L_1 error	L_∞ error
1	0.05	4.975×10^{-3}	1.5	2.648×10^{-4}	1.872×10^{-3}	6.754×10^{-3}	2.168×10^{-1}
2	0.05	4.975×10^{-3}	3.0	7.131×10^{-4}	7.151×10^{-3}	6.864×10^{-3}	2.350×10^{-1}
3	0.05	4.975×10^{-3}	4.5	1.124×10^{-3}	1.311×10^{-2}	6.820×10^{-3}	2.438×10^{-1}
4	0.05	4.975×10^{-3}	6.0	1.931×10^{-3}	4.399×10^{-2}	5.439×10^{-3}	2.900×10^{-1}

For comparison purpose, we take the same initial condition as that presented in [6],

$$u(t=0,\nu) = \begin{cases} -1 & \text{if } \nu < -20 \\ 1 & \text{if } \nu > 20 \\ \dfrac{1}{2}\left(1 - \dfrac{e^{\nu} - e^{-\nu}}{e^{\nu} + e^{-\nu}}\right) & \text{if } -20 \le \nu \le 20, \end{cases} \tag{68}$$

where the new variable ν is defined as $\nu = \frac{x}{4\mu}$. The boundary conditions are prescribed as: given velocity on the left, i.e. $u_{t,-2} = 1$, and outflow condition on the right, i.e. $u_{N+1} - u_N = u_N - u_{N-1}$. The analytical solution to the problem is [6]

$$u(x,t) = 1 - \frac{1}{2}\left(1 - \frac{\exp\left(\frac{0.5t-x}{4\mu}\right) - \exp\left(-\frac{0.5t-x}{4\mu}\right)}{\exp\left(\frac{0.5t-x}{4\mu}\right) + \exp\left(-\frac{0.5t-x}{4\mu}\right)}\right). \tag{69}$$

We use 100 control volumes with $\Delta x = 0.05$. The viscous coefficient is taken as $\mu = 0.05$. For stability consideration, as mentioned previously, τ should satisfy $\tau \le \frac{\mu}{u^2}$. However, in the nonlinear case of viscous Burgers' equation, velocity u is not a constant and it changes with time and location. In our numerical calculation, we use $\tau = \frac{1}{100}\mu$. The stability of the numerical scheme requires that $|\lambda_k|_{\max}\frac{\Delta t}{\Delta x} \le 1$, and we take the maximum allowable time interval, $\Delta t = \frac{\Delta x}{|\lambda_k|_{\max}}$, which results in $\Delta t = 4.975 \times 10^{-3}$. Numerical solutions at $t = 3$ and $t = 4.5$ for viscous coefficient of $\mu = 0.05$ are compared with analytical ones and displayed in Fig. 2(a) and (b), where solid lines represent results of the analytical solution, while the squares represent those of the numerical one.

We then change the viscous coefficient from $\mu = 0.05$ to $\mu = 0.005$, and as a result, the initial condition of u exhibits a discontinuity-like structure. Such a case puts many existing numerical schemes for solving convection–diffusion equations under challenge. As a trial, we developed a numerical code to solve the same problem using a fourth-order accurate discretization in space as the building block and applying the classic fourth-order accurate Runge–Kutta method in time, and it failed to produce the desired solution by exhibiting non-physical oscillations. In contrast, numerical solutions from the present method are stable in simulating discontinuous structures, as shown in Fig. 2(c) and (d). The errors for various combinations of μ and t are listed in Table 3. Compared with Example 1, we do observe relatively larger L_∞ errors, especially for the case of $\mu = 0.005$, due to the fact that a sharp discontinuity-like initial condition is applied, as can be seen from Fig. 2(c) and (d), and a few points diverge from the sharp front. However, in general, the numerical solution agrees with the analytical one fairly well.

Example 3. Two dimension with constant advection velocity.

The two-dimensional convection–diffusion equation with constant advection velocity has been solved by many researchers [9,13,10,11]. An analytical solution in the rectangular domain $x \in [0, 2]$ and $y \in [0, 2]$ with the initial condition of

$$\phi(x,y,0) = \exp\left(-\frac{(x-0.5)^2}{\mu_x} - \frac{(y-0.5)^2}{\mu_y}\right) \tag{70}$$

is given by [13]

$$\phi(x,y,t) = \frac{1}{4t+1}\exp\left(-\frac{(x-ut-0.5)^2}{\mu_x(4t+1)} - \frac{(y-vt-0.5)^2}{\mu_y(4t+1)}\right). \tag{71}$$

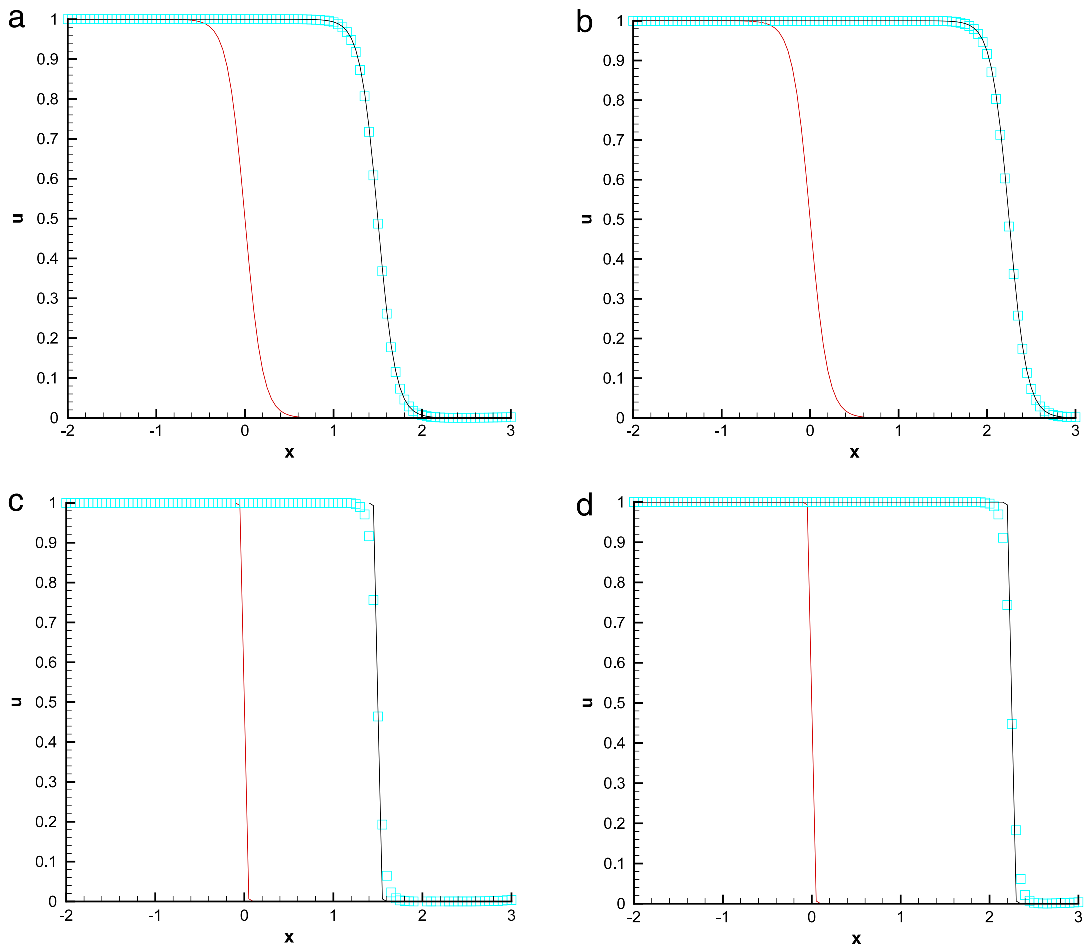

Fig. 2. Solution of 1D viscous Burgers' equation by relaxation method for different viscous coefficients and time. (a) $\mu = 0.05$, $t = 3.0$, (b) $\mu = 0.05$, $t = 4.5$, (c) $\mu = 0.005$, $t = 3.0$, (d) $\mu = 0.005$, $t = 4.5$.

For comparison purpose, we applied our method to the same computational domain and initial condition as in [13]. Our solution is plotted against the analytical one, obtained from Eq. (71), in Fig. 3, where red contours are the initial Gaussian profile, black contours with solid line indicate the numerical solution, while black contours with dash–dot–dot line indicate the analytical solution. Results of two cases are presented, Fig. 3(a) for $\mu = 0.01$, $u = 0.8$, $\Delta x = 0.025$, $\Delta t = 2.5 \times 10^{-3}$, $t = 1.25$, and $\tau = 2.0 \times 10^{-4}$, and Fig. 3(b) for $\mu = 0.01$, $u = 80.0$, $\Delta x = 0.025$, $\Delta t = 2.5 \times 10^{-5}$, $t = 0.0125$, and $\tau = 2.0 \times 10^{-6}$. In both cases, the center of the initial Gaussian pulse moves from $(0.5, 0.5)$ to $(1.5, 1.5)$. Again, good agreement is found between the present method and the exact solution for both cases. We remark that the selection of τ plays an important role in two-dimensional calculation, i.e. it was chosen much smaller than the maximum allowable value. We compared the accuracy of our method with published solutions, as listed in Table 4. We admit that our method is less accurate than You's Padé-ADI method, but competitive if not better than Karaa and Zhang's HOC-ADI and Peaceman and Rachford's PR-ADI methods for the two tested cases. It has been reported by You [11] that both HOC-ADI and PR-ADI methods generated oscillatory solutions in the high velocity case when $u = 80.0$ and $\Delta t = 2.5 \times 10^{-5}$, while ours does not, see Fig. 3(b). It is worth noticing that the ability of handling discontinuous situations has not been reported for the three high-order methods, PR-ADI, HOC-ADI, and Padé-ADI in comparison.

8. Concluding remarks

We developed a numerical method to solve one- and two-dimensional convection–diffusion equations by asymptotic analysis, aimed at removing the second-order derivatives. We solved the asymptotically equivalent relaxation system using high-order accurate characteristic-based methods. Our methods survived rigorous tests involving very large advection velocity, very small viscous coefficient, and nonlinearity. Numerical examples indicate that the proposed method can solve unsteady convection–diffusion equations with sharp discontinuities as well as rich smooth structures effectively, due to

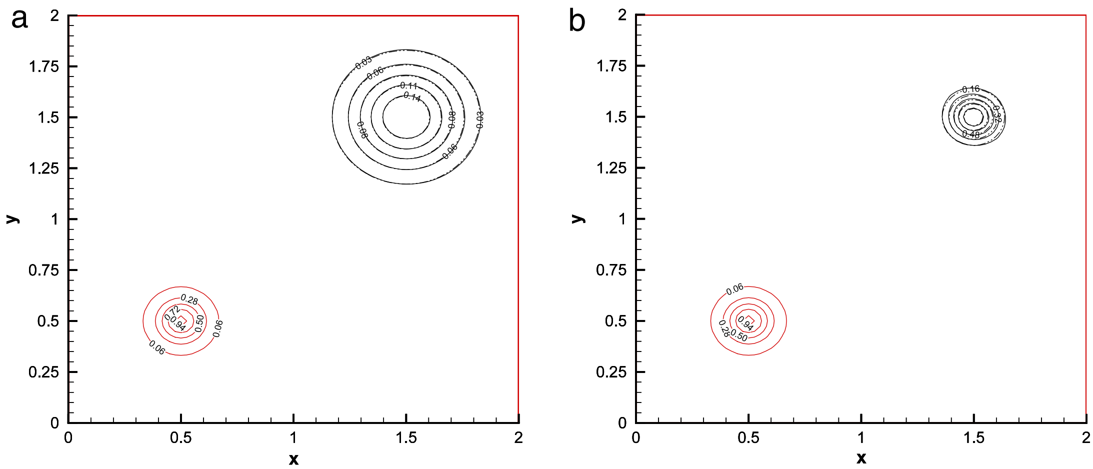

Fig. 3. The transport of a Gaussian profile for various μ and u. (a) Contour plots for $\mu = 0.01$ and $u = 0.8$: contours in red color is the profile of initial Gaussian pulse, while contours in black color is the profile at $t = 1.25$, where the dash–dot–dot line indicates the analytical solution, and the solid line represents the numerical solution. (b) Contour plots for $\mu = 0.01$ and $u = 80.0$: contours in red color is the profile of initial Gaussian pulse, while contours in black color is the profile at $t = 0.0125$, where the dash–dot–dot line indicates the analytical solution, and the solid line represents the numerical solution. (For interpretation of the references to colour in this figure legend, the reader is referred to the web version of this article.)

Table 4
Comparison of L_2 errors among different methods [11].

Method	L_2 errors	
	$\mu = 0.01, u = 0.8$	$\mu = 0.01, u = 80.0$
PR-ADI [10]	$\sim 10^{-5}$	3.29×10^{-4}
HOC-ADI [9]	$\sim 10^{-6}$	1.82×10^{-4}
Padé-ADI [11]	$\sim 10^{-7}$	7.68×10^{-6}
Present method	4.167×10^{-6}	4.126×10^{-5}

third-order discretization in time by the IMEX Runge–Kutta and fifth-order discretization in space by WENO reconstruction. The proposed method can achieve the goal of retaining high-order accuracy in smooth regions and being free of non-physical oscillations in discontinuities for solving linear and nonlinear convection–diffusion equations.

References

[1] R.B. Bird, W.E. Stewart, E.N. Lightfoot, Transport Phenomena, 2nd ed., John Wiley and Sons, New York, 2007.
[2] M. Arora, P.L. Roe, A fresh look at viscous conservation laws via equivalent relaxation systems, in: Proceedings of the 3rd International Congress on Industrial and Applied Mathematics, Hamburg, July 1995.
[3] M. Arora, Explicit Characteristic-based High-resolution Algorithms for Hyperbolic Conservation Laws with Stiff Source Terms, Thesis, The University of Michigan, 1996.
[4] H. Wang, R.E. Wing, G. Qin, S.L. Lyons, M. Al-Lawatia, S. Man, A family of Eulerian–Lagarangian localized adjoint methods for multi-dimensional advection-reaction equations, J. Comput. Phys. 152 (1999) 120–163.
[5] D. Calhoun, R.J. LeVeque, A cartesian grid finite-volume method for the advection-diffusion equation in irregular geometries, J. Comput. Phys. 157 (2000) 143–180.
[6] R.J. LeVeque, Finite Volume Methods for Hyperbolic Problems, Cambridge University Press, 2002.
[7] P.L. Roe, Generalized formulation of TVD Lax-Wendroff schemes, ICASE Report, 1984.
[8] P.K. Sweby, High resolution schemes using flux limiter for hyperbolic conservation laws, SIAM J. Numer. Anal. 21 (1984) 995–1011.
[9] S. Karaa, J. Zhang, High order ADI method for solving unsteady convection–diffusion problems, J. Comput. Phys. 198 (2004) 1–9.
[10] D.W. Peaceman, H.H. Rachford Jr., The numerical solution of parabolic and elliptic differential equations, J. Soc. Ind. Appl. Math. 3 (1959) 28–41.
[11] D. You, A high order Padé ADI method for unsteady convection–diffusion equations, J. Comput. Phys. 214 (2006) 1–11.
[12] B.J. Noye, H.H. Tan, A third-order semi-implicit finite difference method for solving the one-dimensional convection–diffusion equation, Int. J. Numer. Methods Eng. 26 (1988) 1615–1629.
[13] B.J. Noye, H.H. Tan, Finite difference methods for solving the two-dimensional convection–diffusion equation, Int. J. Numer. Methods Fluids 9 (1989) 75–98.
[14] G.-S. Jiang, C.-W. Shu, Efficient implementation of weighted ENO schemes, J. Comput. Phys. 126 (1996) 202–228.
[15] J. Qiu, C.W. Shu, On the construction, comparison, and local characteristics decomposition for high-order central WENO schemes, J. Comput. Phys. 183 (2002) 187–209.
[16] C.W. Shu, Essentially non-oscillatory and weighted essentially non-oscillatory schemes for hyperbolic conservation laws, in: B. Cockburn, C. Johnson, C.W. Shu, E. Tadmor (Eds.), Advanced Numerical Approximation of Nonlinear Hyperbolic Equations, in: Lect. Notes in Math., 1697, Springer-Verlag, Berlin, New York, 1998, p. 325.
[17] T.-P. Liu, Hyperbolic conservation laws with relaxation, Comm. Math. Phys. 108 (1987) 153–175.
[18] L. Pareschi, G. Russo, Implicit-explicit Runge–Kutta schemes and application to hyperbolic systems with relaxation, J. Sci. Comput. 25 (2005) 129–155.
[19] W. Shen, An explicit TVD scheme for hyperbolic heat conduction in complex geometry, Numer. Heat Transfer B 41 (2002) 565–590.